UDK: 629.7.03:621.512:620.178.3
COSATI: 11-13, 20-11

Redesign of Dovetail Joints Based on Estimated Low Cycle Fatigue Life

Strain Posavljak, MSc (Eng)[1)]
Stevan Maksimović, PhD (Eng)[2)]

Fatigue life behavior of the dovetail joint of aero engine axial compressors and its redesigned version were investigated in this work. It is shown how redesigned version increases low cycle fatigue life. It was assumed that elements of joints are made of steel 13H11N2V2MF of known cyclic properties and subjected to blocks of variable force. For the purpose of low cycle fatigue life estimation, the block of variable force was decomposed on the simple cycles. The stress-strain response at critical points, for all simple cycles, was determined using approximate Sonsino's curve, cyclic stress-strain curve and Masing's curve. Stress concentration factors needed for application of the mentioned Sonsino's curve were determined using the finite element method. Palmgren-Miner's rule was applied for damages and low cycle fatigue life estimation.

Key words: **aero engine, compressor, fatigue life, low-cycle fatigue, life cycle, finite elements.**

Introduction

An attention in this work is focused on improving fatigue life properties of aero engine structural components. In aircraft design two approaches can be used: the first require design of structural components without cracks during total life and the second approach deals with allowable cracks in structural components during total life. Fatigue life management of aircraft gas turbine rotors is usually based on a safe life philosophy [5]. The last approach is known as a damage tolerance approach [9-11].

Dovetail joints are mainly applied for disks and blades of aero engine axial compressors. Because of simplified manufacturing, these joints can be seen on disks with narrow and wide rims. Low cycle fatigue (LCF) life of complete disks, in many cases is dependent on LCF life of dovetail joints.

Bad dovetail joints can provoke "premature" cracks and fractures of aero engine disks and blades. If it happens, it is necessary to carry out redesign using estimated LCF life as the key verification parameter.

About a dovetail joint

The joints of blades and stage 1 low-pressure compressor rotor disk of R25-300 aero engine are dovetail joints. This disk made of steel 13H11N2V2MF cannot attain prescribed service life of 1200 flight hours. Because of "premature" cracks in the area of transition rounding at the bottom of the dovetail grooves, the average service life of the mentioned disk amounts approximately to 25% of the prescribed service life [1]. The example of "premature" crack on the observed disk is shown in Fig.1 [2].

It was concluded that the geometry of the existing dovetail joint of the disk with blades was not satisfactory and its redesign was asked for. The aim was to obtain a joint more resistant to LCF. For the sake of simplicity, the joint was reduced to a plane problem. Two types of dovetail joints were discussed, the existing dovetail joint as joint J1 and the redesigned dovetail joint as joint J2. In a different way LCF life of these joints has been analyzed in [3]. The joint J1 loaded by force F is depicted in Fig.2.

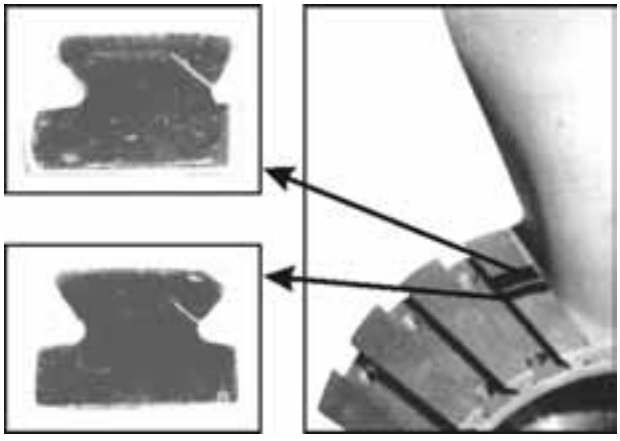

Figure 1. The example of "premature" crack on the observed disk [2]

The difference between joints J1 and J2 is only in the form of lower parts LP1 and LP2. The lower part LP1 has a transition rounding with the radius R1.7 while the lower part LP2 has the transition rounding with the radius R3 (Fig.3). The rounding with the radius R3 is a result of an earlier investigation described in [2].

[1)] Company ORAO Bijeljina, Republic of Srpska, BOSNIA AND HERZEGOVINA
[2)] Military Technical Institute (VTI), Ratka Resanovića 1, 11132 Belgrade, SERBIA

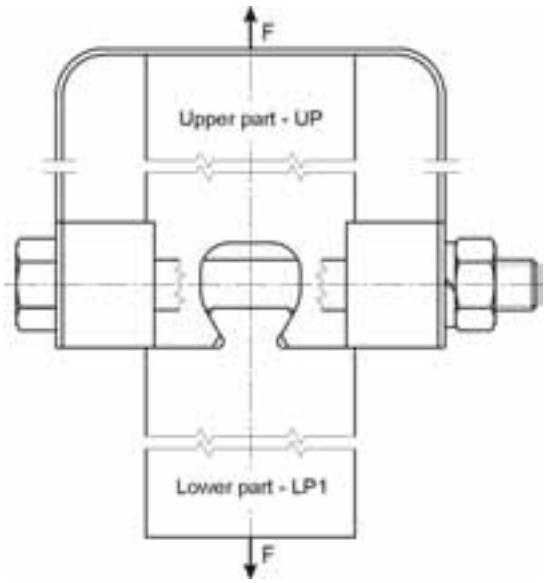

Figure 2. Sketch of joint J1 loaded by force F

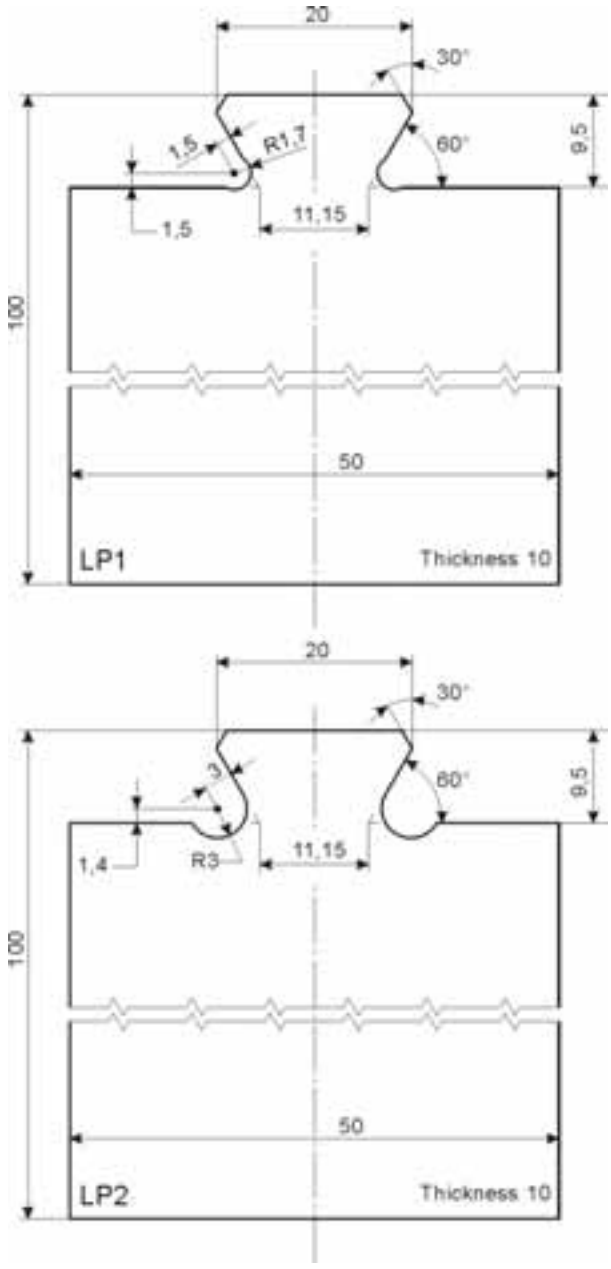

Figure 3. Lower parts LP1 and LP2 of joints J1 and J2

This time, using analytical approach it was necessary to establish that the transition rounding with radius R3 on the lower part LP2 can be applied for increasing of service life of stage 1 of the low pressure compressor rotor disk of R25-300 aero engine. It was assumed that the joints would be loaded by the block of variable force F presented in Fig.4.

For the purpose of estimation of LCF life of the dovetail joints, the block of variable force was modified and decomposed on simple *X-Y-X* force cycles (Fig.5). The levels /*i*/ and numbers /N_i/ of these cycles in the block are given in Table 1. The decomposition of the block of variable force was carried out using the method of "reservoir" [4].

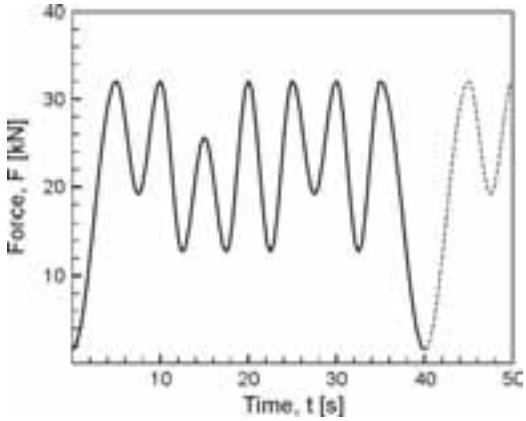

Figure 4. Block of variable force

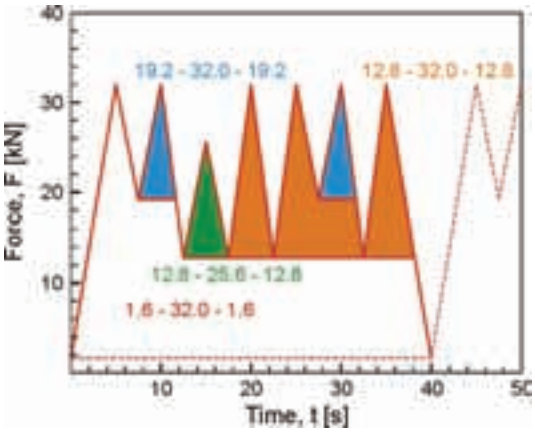

Figure 5. Modified and decomposed block of variable force

Table 1. *X-Y-X* force cycles

Level, *i*	X_i-Y_i-X_i [kN]	Cycles in block N_i
1	1.6-32.0-1.6	1
2	12.8-32.0-12.8	3
3	19.2-32.0-19.2	2
4	12.8-25.6-12.8	1

Table 2. Cyclic properties of quenched and tempered steel 13H11N2V2MF [3]

Property	Value
Modulus of elasticity, *E* [MPa]	229184.6
Cyclic strength coefficient, *K*' [MPa]	1140.0
Cyclic strain hardening exponent, n'	0.0579
Fatigue strength coefficient, σ'_f [MPa]	1557.3
Fatigue strength exponent, *b*	-0.0851
Fatigue ductility coefficient, ε'_f	0.3175
Fatigue ductility exponent, *c*	-0.7214

Material nominated for manufacturing lower and upper parts of dovetail joints is quenched and tempered steel 13H11N2V2MF (heating at 1000°C, oil quenching, tempering at 640°C an air cooling). Cyclic properties of this kind of steel are included in Table 2.

Stress-strain response

At the beginning, the lower parts of the dovetail joints were observed as ideal elastic bodies. The stress response of these parts was obtained using the finite element method (FEM) implemented in I-DEAS Master Series Software. Their symmetrical segments were separated and discretized by plane stress parabolic elements (Fig.6).

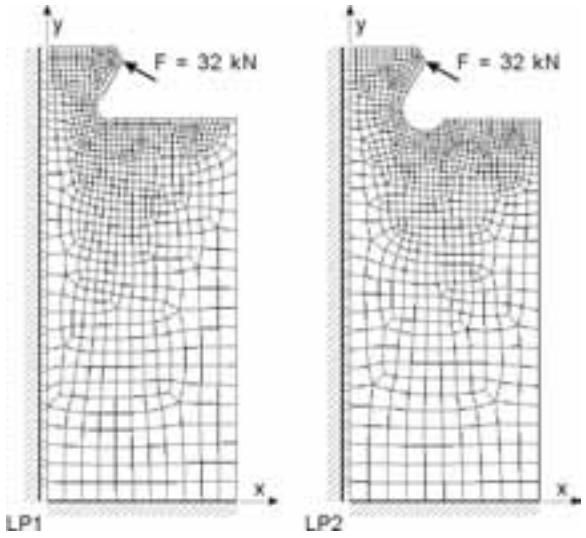

Figure 6. FEM models for stress response calculation of lower parts LP1 and LP2

The maps of the principal stresses σ_1 in Fig.7 were obtained for the most negative case of loading. The contact between lower and upper parts of the dovetail joints was replaced by the nodal force $F = F_{max} = 32$ kN.

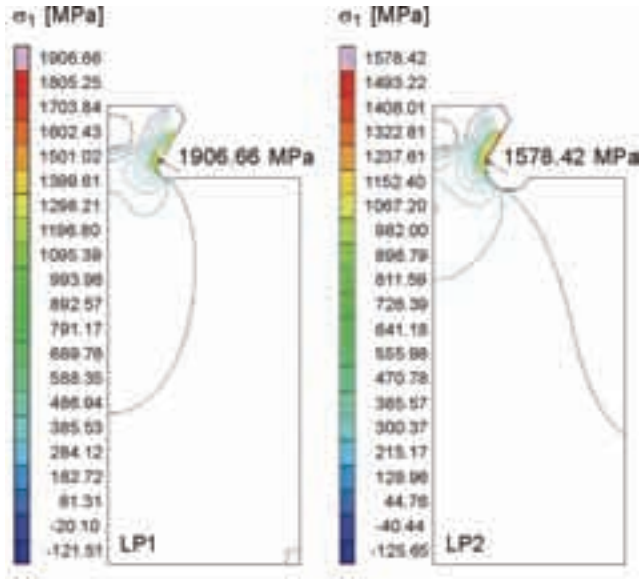

Figure 7. Maps of principal stresses σ_1 of lower parts LP1 and LP2

The principal stress σ_1 has a maximum value at th ecritical points P_1 and P_2 which amount: $\sigma_1(P_1) = 1906.66$ MPa, $\sigma_1(P_2) = 1578.42$ MPa. Positions of these points with acting forces are shown in Fig.8.

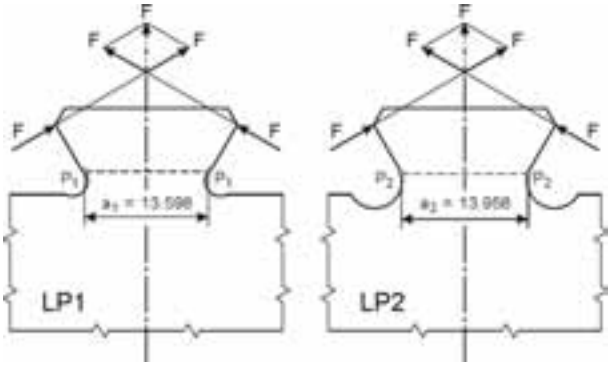

Figure 8. Position of critical points P_1 and P_2 of lower parts LP1 and LP2 with acting forces

The values of nominal stresses $\sigma_{n,1} = 235.33$ MPa and $\sigma_{n,2} = 229.29$ MPa for critical sections defined by points P_1 and P_2 were determined using the following expression

$$\sigma_{n,j} = \frac{F}{A_j} \qquad j = 1,2 \tag{1}$$

where $A_j = a_j \cdot 10$ is the surface of the critical sections at which the resulting force F acts. The stress concentration factors $K_{t,1} = 8.102$ and $K_{t,2} = 6.884$ for the critical sections were determined using the expression

$$K_{t,j} = \frac{\sigma_1(P_j)}{\sigma_{n,j}} \qquad j = 1,2 \tag{2}$$

The real stress-strain response of lower parts LP1 and LP2 of joints J1 and J2, in comparison with the stress-strain response of these parts as ideal elastic bodies is completely different. Namely, their stress-strain response at critical points can be described by stabilized hysteresis loops [5].

The stress-strain response at the critical points of lower part LP1 and *P*2, for the block of variable force, is shown in Fig.9.

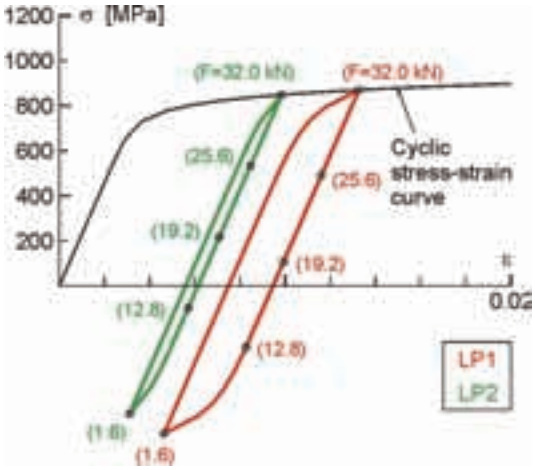

Figure 9. Stress-strain response at the critical points of lower part LP1 and LP2 for the block of variable force

The previous figure shows all stabilized hysteresis loops provoked by X_i-Y_i-X_i force cycles from Table 1.

The upper point as the first point of the stress-strain response corresponding to the force F=32 kN was determined by solving the system of equations

$$\varepsilon = \frac{1}{2}\left(\frac{K_{tj}^2\sigma_{ni,j}^2}{\sigma E} + \frac{K_{tj}\sigma_{ni,j}}{E}\right)$$

$$i = 1 \qquad j = 1,2 \tag{3}$$

$$\varepsilon = \frac{\sigma}{E} + \left(\frac{\sigma}{K'}\right)^{\frac{1}{n'}}$$

The dimensions ($\Delta\varepsilon$ x $\Delta\sigma$) of the stabilized hysteresis loops were determined using the following equation system

$$\varepsilon = \frac{1}{2}\left(\frac{K_{tj}^2 \Delta\sigma_{ni,j}^2}{\Delta\sigma E} + \frac{K_{tj}\Delta\sigma_{ni,j}}{E}\right)$$

$$i = 1,2,3,4 \quad j = 1,2 \tag{4}$$

$$\Delta\varepsilon = \frac{\Delta\sigma}{E} + 2\left(\frac{\Delta\sigma}{2K'}\right)^{\frac{1}{n'}}$$

The first equations in systems (3) and (4) are two forms of the approximate Sonsino's curve, while the second equations in that systems are equations of the cyclic stress-strain curve and Masing's curve of quenched and tempered steel 13H11N2V2MF. The mentioned systems were solved graphically using the Drafting module of I-DEAS Master Series Software. The cyclic stress-strain curve, Masing's curve and the approximate Sonsino's curves were copied into corresponding spline curves by special Fortran programs. The position of stabilized hysteresis loops was determined using memory of metals. Masing's curve served for their modeling. The values for E, K' and n' in systems (3) and (4) were taken from Table 2. For the stress concentration factors K_{tj} (j = 1,2), the already determined values K_{t1} = 8.102 and K_{t2} = 6.884 were taken. The values of nominal stresses $\sigma_{ni,j}$ and nominal stress ranges $\Delta\sigma_{ni,j}$ for critical sections were taken from Table 3. These values were obtained by expressions

$$\sigma_{ni,j} = \frac{Y_i \cdot 10^3}{A_j}$$

$$\text{i} = 1,2,3,4 \quad \text{j} = 1,2 \tag{5}$$

$$\Delta\sigma_{ni,j} = \frac{(Y_i - X_i)\cdot 10^3}{A_j}$$

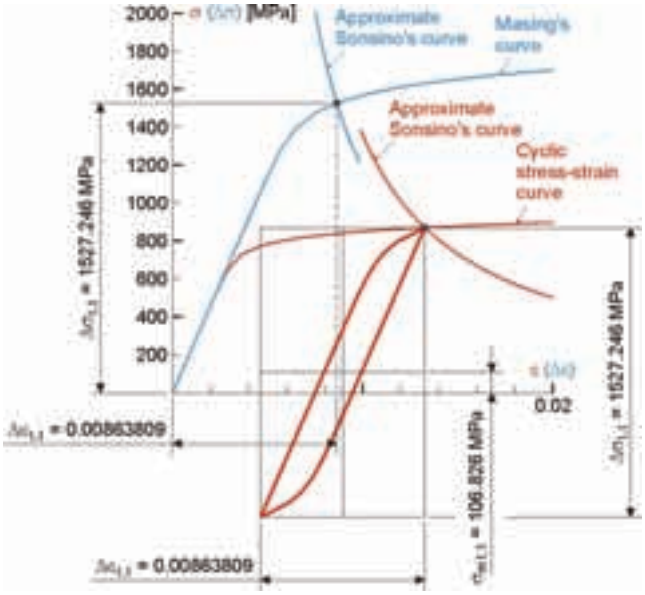

Figure 10. Stress-strain response at the critical point of lower part LP1 for 1.6-32.0-1.6 force cycle

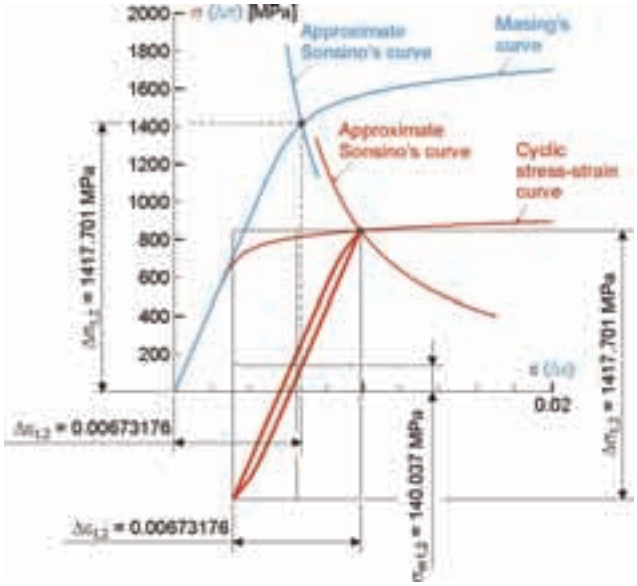

Figure 11. Stress-strain response at the critical point of lower part LP2 for 1.6-32.0-1.6 force cycle

Table 3. Values of nominal stresses and nominal stress ranges for critical sections

i	X_i-Y_i-X_i [kN]	Lower part LP1		Lower part LP2	
		$\sigma_{ni,1}$	$\Delta\sigma_{ni,1}$	$\sigma_{ni,2}$	$\Delta\sigma_{ni,2}$
1	1.6-32.0-1.6	235.33	223.56	229.29	217.83
2	12.8-32.0-12.8	235.33	141.20	229.29	137.58
3	19.2-32.0-19.2	235.33	94.13	229.29	91.72
4	12.8-25.6-12.8	188.26	94.13	183.43	91.72

The graphically determined stress-strain responses at critical points of lower parts LP1 and LP2 for 1.6-32.0-1.6 force cycles are given in Fig.11 and Fig.12.

The complete numerical results of the stress-strain response at the critical points of lower parts LP1 and LP2 described by stabilized hysteresis loops for all force cycles are included in Table 4 and Table 5.

Table 4. Numerical results of the stress-strain response for the critical point of lower part LP1

i	X_i-Y_i-X_i [kN]	$\sigma_{mi,1}$	$\Delta\sigma_{i,1}$	$\Delta\varepsilon_{i,1}$
1	1.6-32.0-1.6	106.826	1527.246	0.00863809
2	12.8-32.0-12.8	299.443	1142.012	0.00499597
3	19.2-32.0-19.2	489.127	762.644	0.00332765
4	12.8-25.6-12.8	109.759	762.644	0.00332765

Table 5. Numerical results of the stress-strain response for the critical point of lower part LP2

i	X_i-Y_i-X_i [kN]	$\sigma_{mi,2}$	$\Delta\sigma_{i,2}$	$\Delta\varepsilon_{i,2}$
1	1.6-32.0-1.6	140.037	1417.701	0.00673176
2	12.8-32.0-12.8	375.376	947.023	0.00413267
3	19.2-32.0-19.2	533.189	631.398	0.00275500
4	12.8-25.6-12.8	217.564	631.398	0.00275500

Equations of approximate Sonsino's curves in systems (3) and (4) were derived here on the basis of Sonsino's modification of the local stress-strain response of notched elements, determined using a famous Neuber's hyperbola [5]

$$\sigma\varepsilon = \frac{K_t^2 \sigma_n^2}{E} \tag{6}$$

Sonsino's modification of Neuber's rule, illustrated in Fig.12, was explained in paper [6].

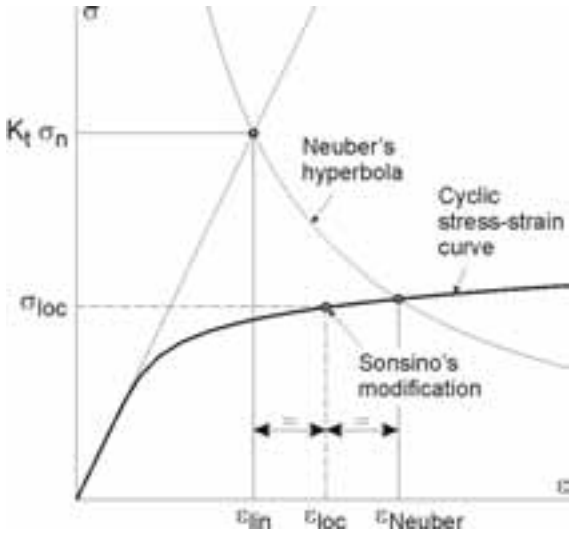

Figure 12. Sonsino's modification of Neuber's rule

The expression for local strain according to Fig.10 has a form

$$\varepsilon_{loc} = \frac{\varepsilon_{lin} + \varepsilon_{Neuber}}{2} \tag{7}$$

where linear strain

$$\varepsilon_{lin} = \frac{K_t \sigma_n}{E} \tag{8}$$

The already mentioned equations of approximate Sonsino's curves in systems (3) and (4) are practically derived with the help of expression (7) including (6) and (8) in it.

Estimation of damage and low cycle fatigue life

Estimation of damage D_B caused by the block of variable force was carried out using Palmgren-Miner's rule of linear damage accumulation [4,5,7,9] in the form

$$D_{B,j} = \sum_{i=1}^{4} D_{i,j} = \sum_{i=1}^{4} \frac{N_i}{N_{fi,j}} \qquad j = 1,2 \tag{9}$$

The numbers of N_i of X_i-Y_i-X_i force cycles were taken from Table 1, while the numbers of cycles to crack initiation $N_{fi,j}$ were obtained using system equations

$$\frac{\Delta\varepsilon}{2} = \frac{\sigma_f' - \sigma_{mi,j}}{E} N_f^b + \varepsilon_f' N_f^c$$

$$i = 1,2,3,4 \quad j = 1,2 \tag{10}$$

$$\frac{\Delta\varepsilon}{2} = \frac{\Delta\varepsilon_{i,j}}{2}$$

where the first equation presents different Morrow's curves [5,8].

System equation (10) was solved also graphically using the Drafting module of I-DEAS Master Series Software. Morrow's curves were copied into corresponding spline curves by a special Fortran program. Mean stress values $\sigma_{mi,j}$ and strain range values $\Delta\varepsilon_{i,j}$ were taken from Table 4 and Table 5. For example, the determination of the number of cycles to crack initiation on lower part LP1, for 1.6-32.0-1.6 force cycle, is shown in Fig.13.

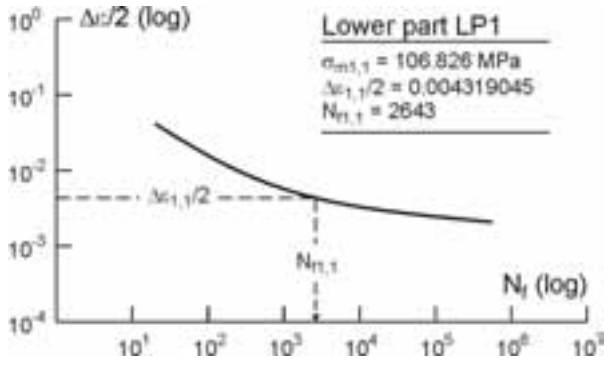

Figure 13. Determining the number of cycles to crack initiation on lower part LP1 for 1.6-32.0-1.6 force cycles

The numbers of cycles to crack initiation $N_{fi,j}$, damage $D_{i,j}$ caused by all X_i-Y_i-X_i force cycles, including damage $D_{B,j}$ caused by the block of variable force, are contained in Table 6 and Table 7. These tables contain also values of LCF life (LCFL) as reciprocal values of damage caused by the block.

Table 6. Lower part LP1: $N_{fi,1}$ / $D_{i,1}$ / $D_{B,1}$ / $LCFL_1$

i	X_i-Y_i-X_i [kN]	N_i	$N_{fi,1}$	$D_{i,1}$
1	1.6-32.0-1.6	1	2643	0.000378358
2	12.8-32.0-12.8	3	27566	0.000108830
3	19.2-32.0-19.2	2	242808	0.000008237
4	12.8-25.6-12.8	1	6599058	0.000000152
$D_{B,1}$				0.000495576
$LCFL_1 = 1/D_{B,1}$ [Block]				2017

Table 7. Lower part LP2: $N_{fi,2}$ / $D_{i,2}$ / $D_{B,2}$ / $LCFL_2$

i	X_i-Y_i-X_i [kN]	N_i	$N_{fi,2}$	$D_{i,2}$
1	1.6-32.0-1.6	1	7967	0.000125518
2	12.8-32.0-12.8	3	79641	0.000037669
3	19.2-32.0-19.2	2	1137703	0.000001758
4	12.8-25.6-12.8	1	24102716	0.000000041
$D_{B,2}$				0.000164986
$LCFL_2 = 1/D_{B,2}$ [Block]				6061

The histogram of LCF life data of lower parts LP1 and LP2 is presented in Fig.14.

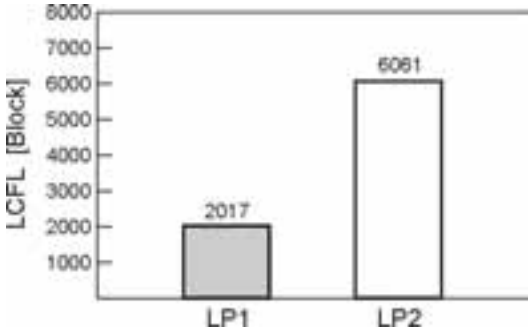

Figure 14. Histogram of LCF life of lower part LP1 and LP2

Conclusion

This paper presents complete computation procedures including redesign of structural components to improve their fatigue life. Attention in this investigation is focused on aircraft aero engine structural components but the computation procedure is of a general type.

On the basis of estimated LCF life it can be concluded that the transition rounding on the lower part LP2 of the dovetail joint J2, with radius R3 can be applied for a new dovetail joint of blades and stage 1 low pressure compressor rotor disk of R25-300 aero engine. A new disk with this transition loading at the bottom of dovetail grooves could have considerably longer service life.

References

[1] RADOJKOVIC,R.: *Reliability of Vital Rotating Parts of Turbojet Engines*, Seminar paper, Aeronautic Military Academy, Belgrade – Zarkovo, 1992 (in Serbian).

[2] POSAVLJAK,S.: *Stress-strain Analysis and Fatigue of Materials of Turbojet Engine*, Master Thesis, Belgrade University, Mechanical Faculty, 1999 (in Serbian).

[3] POSAVLJAK,S.: *Low Cycle Fatigue Life Estimation of Dove Tail Joints*, Proceedings, 1st International Congress of Serbian Society of Mechanics, 10-13th April, 2007, Kopaonik. pp. 723-730.

[4] KOSTAES,D.: *Fatigue Behavior and Analysis*, Talat Lecture 2401, Technische Universität München, EAA – European Aluminum Association, 1994.

[5] BANNATINE,J.A., COMMER,J., HANDROCK,J.: *Fundamentals of Material Fatigue Analysis*, Prentice-Hall, Englewood Cliffs, New Jersey, 1990.

[6] SONSINO,C.M.: *Zur Bewertung des Schwingfestig-keitsverhaltens von Bauteilen mit Hilife örtlicher Baunspruchungen*, Konstruktion 45 (1993) 25-33.

[7] FATEMY,A., YANG,L.: *Cumulative fatigue damage and prediction theories: a survey of the state of the art for homogeneous materials*, International Journal of Fatigue, Vol. 20, No. 1, 1988, pp. 9-34.

[8] MORROW,J.: *Fatigue Design Handbook*, Advances in Fatigue, Vol. 4, Society of Automotive Engineers, Warrendale, Pa., 1968, Sec 3.2, pp. 21-29.

[9] MAKSIMOVIĆ,S.: *Fatigue Life Analysis of Aircraft Structural Components*, Scientific Technical Review, Scientific Technical Review, 2005, Vol.LV, No.1, pp.15-22.

[10] MAKSIMOVIĆ,K., NIKOLIĆ-STANOJEVIĆ,V., MAKSIMOVIĆ,S.: *Modeling of the surface cracks and fatigue life estimation*, ECF 16, 16th European Conference of Fracture, ECF 16, Alexandroupolis, Grčka, 2006

[11] MAKSIMOVIĆ,S., BURZIĆ,Z., MAKSIMOVIĆ,K.: *Fatigue life estimation of notched structural components*: Computation and Experimental Investigations, 16th European Conference of Fracture, ECF 16, Alexandroupolis, Grčka, 2006

Received: 10.10.2008.

Reprojektovanje vitalnih veza na bazi procene veka u području niskocikličnog zamora

U radu je razmatran problem ponašanja na zamor vitalne veze u vidu lastinog repa kod kompresora avionskog motora kao i njeno reprojektovanje. Prikazano je kako se reprojektovanjem odnosno optimizacijom oblika, može izvršiti povećanje njenog veka u domenu niskocikličnog zamora. Bilo je predpostavljeno da je vitalna veza izrađena od čelika 13H11N2V2MF za koga su eksperimentalno određene ciklične karakteristike pod dejstvom spektra opterećenja promenljivih amplituda i definisanih u vidu blokova opterećenja. Zavisnosti između napona i deformacije u kritičnoj tački vitalne veze, za sve pravilne cikluse, su određene koristeći aproksimativnu Sonsinovu krivu, cikličnu krivu napon-deformacija i Mazingovu krivu. Faktor koncentracije napona koji je neophodan za pomenutu Mazingovu krivu određen je primenom metode konačnih elemenata. Palmgren-Majnerovo pravilo bilo je korišćeno za sračunavanje oštećenja i procena veka u domenu niskocikličnog zamora.

Ključne reči: **avionski motor, kompresor, zamor materijala, niskociklični zamor, vek trajanja, konačni element.**

Перепроектирование соединений ласточкиным хвостом на основании оценки века (срока службы) в области усталости низкого цикла

В настоящей работе рассматривана проблема поведения на усталость соединений ласточкиным хвостом у компрессоров самолётного двигателя, а в том числе и их перепроектирования. Здесь показано, как перепроектированием, т.е. оптимизацией формы, возможно увеличить их век (срок службы) в области усталости низкого цикла. Уже предположено, что соединение ласточкиным хвостом сделано из стали 13Х11Н2В2МФ, для которой уже экспериментально определены циклические характеристики под влиянием спектра нагрузки переменчивых амплитуд и определённых в виду блоков нагрузки. Зависимости между напряжением и деформациями в критической точке соединения ласточкиным хвостом определены для всех правильных циклов с использованием аппроксимативной кривой Сонсина, циклической кривой напряжение-деформация и кривой Масинга. Фактор концентрации напряжения, необходимый для упомянутой кривой Масинга, определён применением метода конечных элементов. Правило Палмгрен-Минера было использовано для подсчитывания ущерба и оценки века (срока службы) в области усталости низкого цикла.

Ключевые слова: **самолётный двигатель, компрессор, усталость материала, усталость низкого цикла, срок службы, конечный элемент.**

Modification du projet des assemblages basée sur l'estimation de la durée de vie dans le domaine de la fatigue basse cyclique

Le problème du comportement quant à la fatigue de l'assemblage en forme de queue d'aronde chez le compresseur du moteur d'avion ainsi que sa modification sont considérés dans cet article. On a exposé comment un projet modifié,c'est-à-dire l'optimisation de sa forme, peut augmenter la durée de sa vie dans le domaine de la fatigue basse cyclique. On a supposé que l'assemblage était réalisé en acier 13H11N2V2MF dont les propriétés cycliques ont été déterminées par la voie expérimentale sous l'action du spectre de charge des amplitudes variables et définies en forme de blocs charges. Les dépendances entre la tension et les déformations dans le point critique de l'assemblage, pour tous les cycles réguliers, ont été déterminées au moyen de la courbe de Sonsino, la courbe cyclique tension - déformation et la courbe de Masing. Le facteur de la concentration de la tension, nécessaire à la courbe de Masing, a été déterminé par la méthode des éléments finis. On a employé le règlement de Palmgren - Miner pour calculer l'endommagement et l'estimation de la durée de vie dans le domaine de la fatigue basse cyclique.

Mots clés: **moteur d'avion, compresseur, fatigue de matériel, fatigue basse cyclique durée de vie, élément fini.**